ELSEVIER

Physica C 351 (2001) 386–394

PHYSICA C

www.elsevier.nl/locate/physc

Polarized far-infrared and Raman spectra of $SrCuO_2$ single crystals

Z.V. Popović [a,b,*], M.J. Konstantinović [a,c], R. Gajić [a], C. Thomsen [d], U. Kuhlmann [d], A. Vietkin [e]

[a] *Institute of Physics, P.O. Box 68, 11080 Belgrade, Yugoslavia*
[b] *Laboratorium voor Vaste-Stoffysica en Magnetisme, K.U. Leuven, Celestijnenlaan 200D, B-3001 Leuven, Belgium*
[c] *Max-Planck-Institut für Festkörperforschung, Heisenbergstrasse 1, D-70569 Stuttgart, Germany*
[d] *Institut für Festkörperphysik, Technische Universität Berlin, Hardenbergstrasse 36, D-10623 Berlin Germany*
[e] *Department of Physics, Moscow State University, 119899 Moscow, Russia*

Received 7 July 2000; received in revised form 2 October 2000; accepted 10 October 2000

Abstract

We measured polarized far-infrared reflectivity and Raman scattering spectra of $SrCuO_2$ single crystals. The frequencies for infrared-active modes were determined using an oscillator-fitting procedure of reflectivity data. The Raman spectra were measured at different temperatures using several laser energies ω_L. In addition to eight of twelve Raman active modes, predicted by factor-group analysis, we observed a complex structure in the Raman spectra for polarization parallel to the *c*-axis, which consists of Raman-allowed A_g symmetry modes, and B_{1u} LO infrared-active (Raman-forbidden) modes of the first and higher order as well as their combinations. The Raman-forbidden modes have a stronger intensity at higher ω_L than the Raman-allowed ones. In order to explain this resonance effect, we measured the dielectric function and optical reflection spectra of $SrCuO_2$ in the visible range. We show that the Raman-allowed A_g symmetry modes are resonantly enhanced when a laser energy is close to E_0, while Raman-forbidden (IR-active) modes resonate strongly for laser line energies close to the electronic transition of higher energy gaps. © 2001 Elsevier Science B.V. All rights reserved.

PACS: 78.30.Hv; 78.20.Ci; 63.20.Dj; 71.27.+a

1. Introduction

Strontium copper oxide belongs to the new family of 1D antiferromagnetic insulators the properties of which have been subject of intensive studies in recent years [1–8]. This oxide, grown in single crystalline form under ambient conditions, has an orthorhombic unit cell (space group D_{2h}^{17}: Cmcm) with parameters $a = 0.3577$ nm, $b = 1.6342$ nm, $c = 0.39182$ nm and $Z = 4$ [9,10]. The compound has a unique structure consisting of CuO_4 squares, mutually connected via common edges that form double copper chains (Fig. 1). These double chains, stretched along the *c*-axis, could be taken as a quasi-one-dimensional antiferromagnetic chains of

* Corresponding author. Present address: Laboratorium voor Vaste-Stoffysica en Magnetisme, K.U. Leuven, Celestijnenlaan 200D, B-3001 Leuven, Belgium. Tel.: +32-16-327-118; fax: +32-16-327-983.

E-mail address: zoran.popovic@fys.kuleuven.ac.be (Z.V. Popović).

0921-4534/01/$ - see front matter © 2001 Elsevier Science B.V. All rights reserved.
PII: S0921-4534(00)01636-1

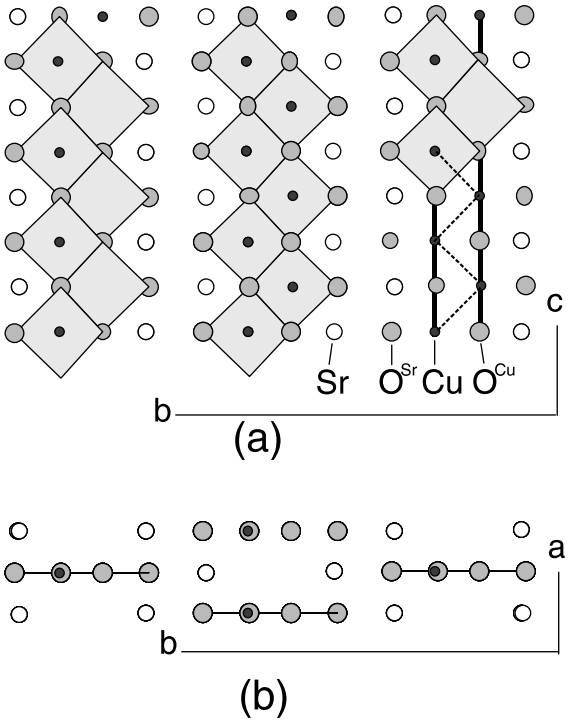

Fig. 1. Schematic representation of the $SrCuO_2$ crystal structure.

Cu^{2+} ions with $S = 1/2$, since the 90° Cu–O–Cu superexchange interactions between neighboring chains is negligible in comparison with the 180° Cu–O–Cu superexchange interactions along the chains [2]. Magnetic susceptibility measurements of $SrCuO_2$ show that the Cu^{2+} moments order antiferromagnetically at about 2 K [4]. The exchange interaction energy J is estimated to be 2100 ± 200 K [5].

The Raman scattering spectra of $SrCuO_2$ were reported in Ref. [6]. The A_g symmetry modes at 188, 262, 543 and 558 cm^{-1} were clearly resolved at room temperature. The Raman spectra for the polarization parallel to Cu–O chains show additional structures ascribed to either phonons strongly coupled to spinons or pairs of unbound spinons that resonate as the excitation energy approaches the charge-transfer (CT) gap [6].

More recently [7,8], micro-Raman and the far-infrared (FIR) measurements of polycrystalline $SrCuO_2$ were reported. The assignment of the observed modes was given according to a shell model lattice-dynamics calculation [7]. In addition to the Raman-allowed modes, numerous lines with A_g symmetry appear for polarization parallel to the Cu–O chains only. These modes originate from the B_{1u} LO modes and their overtones and combinations, becoming Raman-active via Fröhlich interaction [8]. It was also shown in Ref. [8], using the calculated combination two-phonon density of states of only B_{1u} dispersion curves, that non-phonon excitations [6] are not necessary for the understanding of Raman spectra on $SrCuO_2$. Infrared and Raman unpolarized spectra of the tetragonal modification of this oxide have been analyzed in Ref. [11]. Some of our preliminary results we discussed in Ref. [12].

In this paper we report measurements of the FIR reflectivity and Raman scattering spectra of single crystal $SrCuO_2$, which enables us to make full use of polarization selection rules. The TO and LO frequencies of B_{1u}, B_{2u} and B_{3u} infrared-active modes were obtained by applying an oscillator-fitting procedure to the reflectivity data. The Raman spectra were measured at 10 K and at room temperature. Eight Raman active modes of different symmetry were resolved. The Raman spectra for polarization along the Cu–O chains show a rich structure consisting of Raman-allowed A_g symmetry modes and B_{1u} LO infrared-active (Raman-forbidden) modes of the first and higher order as well as their combinations. These modes become more pronounced when Ar laser lines of higher photon energy are used. In order to explain this resonant effect, we analyzed optical properties of this oxide in the visible range on the basis of optical reflection and dielectric function measurements.

2. Experimental details

The present work was performed using single crystal sample with a size of about 20, 3 and 7 mm along the *a*, *b* and *c* axes, respectively. The Raman spectra were measured in the backscattering configuration using Ar and Kr lasers for excitation sources. For low temperature measurements we used a closed-cycle cryostat. The scattered light was detected by a Jobin Yvon U-1000 (XY-800

Dilor) double (triple) monochromator with 1800 groove/mm gratings and a RCA 31034 A photomultiplier (CCD) as a detector. The FIR reflectivity measurements were carried out with a BOMEM DA-8 FIR spectrometer. A DTGS pyroelectric detector was used to cover the wave number region from 100 to 700 cm^{-1}. The spectra were collected with the 2 cm^{-1} resolution. We measured the pseudodielectric function with a help of a rotating-analyzer ellipsometer. A Xe-lamp was used as a light source, a double monochromator with 1200 lines/mm gratings and an S20 photomultiplier tube as a detector. The polarizer and analyzer were Rochon prisms. The measurements were performed in the 1.2–5.6 eV energy range. Optical reflectivity was measured in the 200–2500 nm spectral range using Perkin–Elmer, model Lambda spectrophotometer.

3. Results and discussion

Room temperature polarized FIR reflectivity spectra of $SrCuO_2$, in the spectral range from 100 to 675 cm^{-1}, are shown in Fig. 2. The circles are the experimental data and the solid lines represent the spectra computed using a four-parameter model for the dielectric constant:

$$\varepsilon(\omega) = \varepsilon_\infty \prod_{j=1}^{n} \frac{\omega_{\mathrm{LO},j}^2 - \omega^2 + \mathrm{i}\gamma_{\mathrm{LO},j}\omega}{\omega_{\mathrm{TO},j}^2 - \omega^2 + \mathrm{i}\gamma_{\mathrm{TO},j}\omega}, \tag{1}$$

where $\omega_{\mathrm{LO},j}$ and $\omega_{\mathrm{TO},j}$ are longitudinal and transverse frequencies of the jth oscillator, $\gamma_{\mathrm{LO},j}$ and $\gamma_{\mathrm{TO},j}$ are their corresponding dampings, and ε_∞ is the high-frequency dielectric constant. The best-oscillator-fit parameters are listed in Table 1. The static dielectric constant, given in Table 1, was obtained using the generalized Lyddane–Sachs–Teller relation:

$$\varepsilon_0 = \varepsilon_\infty \prod_{j=1}^{n} \frac{\omega_{\mathrm{LO},j}^2}{\omega_{\mathrm{TO},j}^2}. \tag{2}$$

As can be seen in Fig. 2, the agreement between the observed and the calculated reflectivity spectra is satisfactory. Deviations between these spectra occurs only there where the leakage from another polarization exists.

The factor-group analysis for this crystal predicts:

$$\Gamma_{SrCuO_2} = 4A_g(aa, bb, cc) + 4B_{1g}(ab) + 4B_{3g}(bc) + 3B_{1u}(E||c) + 3B_{2u}(E||b) + 3B_{3u}(E||a). \tag{3}$$

According to Fig. 2 and Table 1, all nine infrared active modes are observed. Comparing our single crystal reflectivity spectra with those previously published for polycrystalline samples (Table 1), we found a difference between the TO(LO) frequencies which, for higher energy modes, reaches a value of 10 (25) cm^{-1}. Such a big difference may be expected because the reflectivity measurements carried out on polycrystalline samples give good results for TO and LO mode frequencies in the case of isolated oscillators only. Here we have different symmetry oscillators with almost identical TO and different LO frequencies. It is not possible, therefore, to extract precise values of the optical parameters either by Kramers–Kronig analysis or oscillator-fitting procedure from the unpolarized reflectivity spectra (see inset in Fig. 2).

We also measured the unpolarized reflectivity spectra at low temperature of 10 K. Note the strong frequency shift of the LO_3 mode from 586 to 596 cm^{-1} upon lowering the temperature to 10 K (dashed curve in inset in Fig. 2). No evidence of any additional structure was observed.

The polarized Raman scattering spectra of $SrCuO_2$ measured at room temperature are shown in Fig. 3. According to the assignments given in Ref. [7], the lowest frequency A_g mode at 186 cm^{-1} originates from the vibration of Sr atoms; the mode at 262 cm^{-1} represents Cu vibrations, while the other two A_g high frequency modes are assigned to O^{Sr} and O^{Cu} vibrations, respectively. Let us note that the polarization dependence of the strength of the A_g modes, shown for blue excitation at 488 nm in Fig. 3, disappears for the red excitation of the Kr laser at 647.1 nm. Namely, the A_g modes at 186 and 262 cm^{-1} are nearly of the same intensity for the 647.1 nm excitation at 300 K.

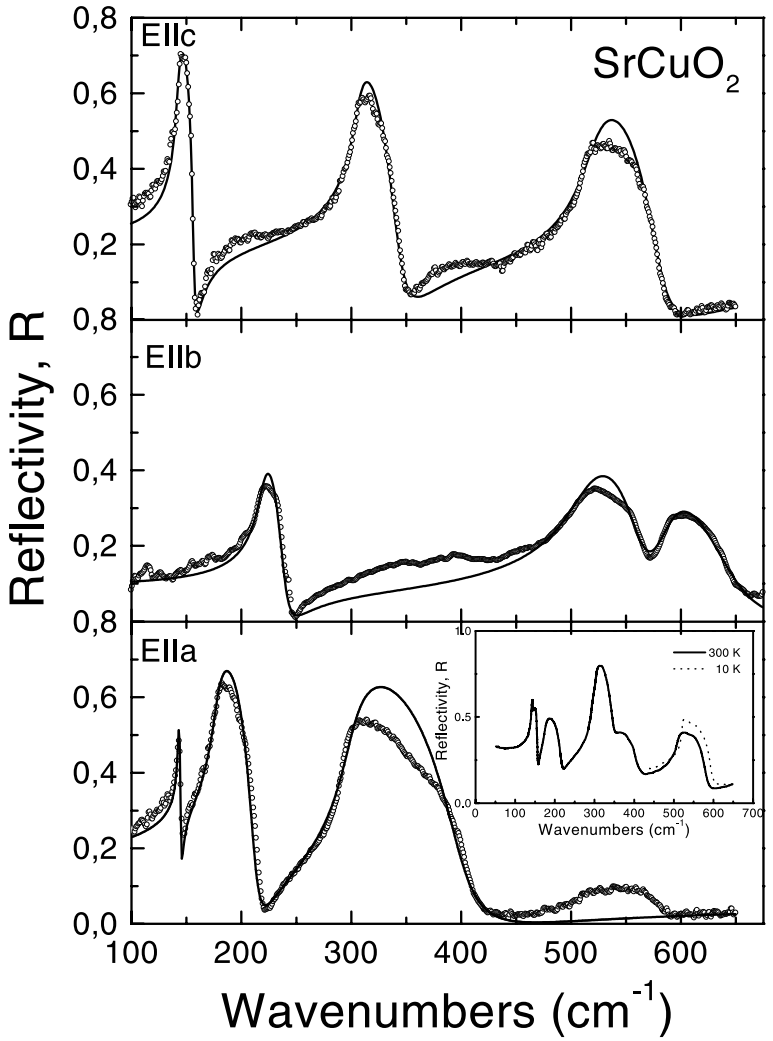

Fig. 2. Room temperature polarized FIR reflectivity spectra of $SrCuO_2$ single crystal in the spectral range 100–675 cm^{-1} for all three principal polarizations. The experimental values are given by open circles. The solid lines represent the calculated spectra obtained by a fitting procedure described in text. Inset: unpolarized reflectivity spectra of $SrCuO_2$ single crystal at room temperature (—) and 10 K (- - -).

The Raman spectra for crossed polarization are shown in the Inset of Fig. 3. The B_{1g} symmetry modes can be seen for (xy) polarization. For this polarization we clearly observed the Cu vibration mode at about 150 cm^{-1} and O^{Sr} vibration mode at 229 cm^{-1}. We observed also a wide structure at about 215 cm^{-1} which represents a superposition of two peaks at 211 and 217 cm^{-1}. The peak at 217 cm^{-1} is the mode of B_{3g} symmetry. Thus we identified three of four B_{1g} modes. The fourth mode of this symmetry was observed at 78 cm^{-1} in Ref. [7]. Very strong rotational modes of nitrogen from air do not allow us to resolve this mode in our experiment here. For (zy) polarization we found only one mode at about 217 cm^{-1}, which represents Cu vibrations [7]. Other modes of this symmetry are probably of very week intensity.

The Raman spectra of $SrCuO_2$ for the (cc) polarization configuration (incident and scattered light are polarized along the Cu–O chains) at 10 K

Table 1
Frequencies and dampings (in cm^{-1}) of infrared and Raman active modes in $SrCuO_2$

Polarization	ω_{TO}	Ref. [7]	γ_{TO}	ω_{LO}	Ref. [7]	γ_{LO}	ε_∞	ε_0
	142.5	(148)	5	157	(154)	4		
$E \| c$	307	(291)	13	345	(370)	25	4	7.7
	520	(506)	30	582	(561)	30		
	200	–	15	221	–	15		
$E \| b$	506	–	50	560	–	40	2	3.7
	580	(577)	40	645	(527)	70		
	143	(137)	2	145	(146)	2		
$E \| a$	178	(172)	12	213	(218)	15	2.5	6.5
	300	–	25	400	–	40		
A_g:	186	(188)	B_{1g}:	–	78	B_{3g}:	–	(120)
	262	(263)		150	(150)		217	(219)
	543	(544)		211	–		–	(320)
	558	(560)		229	(231)		–	–

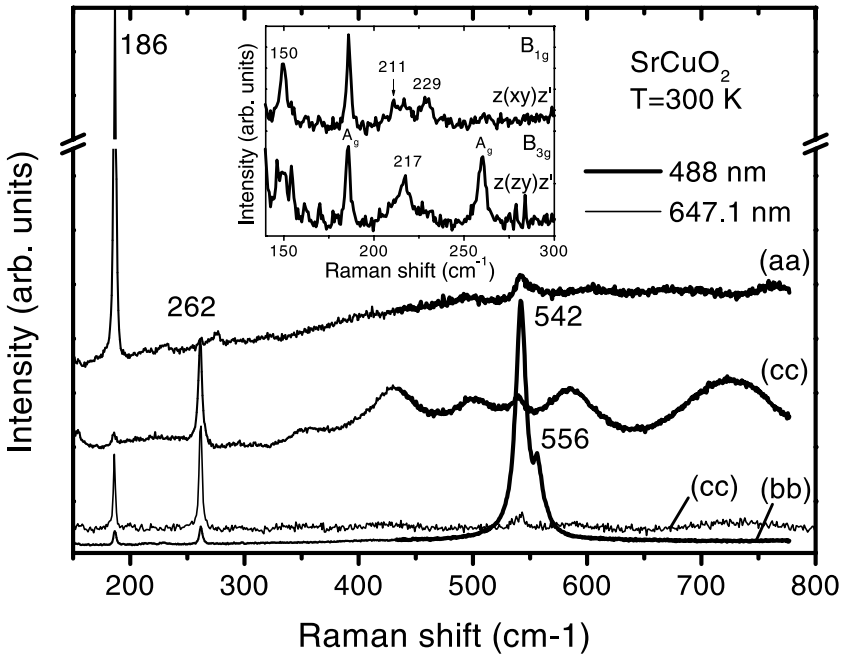

Fig. 3. Raman scattering spectra of $SrCuO_2$ at room temperature for different polarization configurations. Inset: B_{1g} and B_{3g} scattering configuration; the A_g modes appear through leakage.

are shown in Fig. 4. These spectra consist of Raman-allowed A_g symmetry modes and Raman-forbidden–infrared-active B_{1u} LO modes, their overtones and combinations, becoming Raman-active via Fröhlich interaction [8]. Appearance of the infrared active modes in the Raman spectra of CuO based materials is observed when the laser energy is close to the charge-transfer (CT) gap transition [13–16]. It was shown [14] that, depending on coordination, the values of the CT gap decrease from 2.0 eV in the case of octahedral CuO_2 layers in La_2CuO_4 to 1.5 eV in square-type

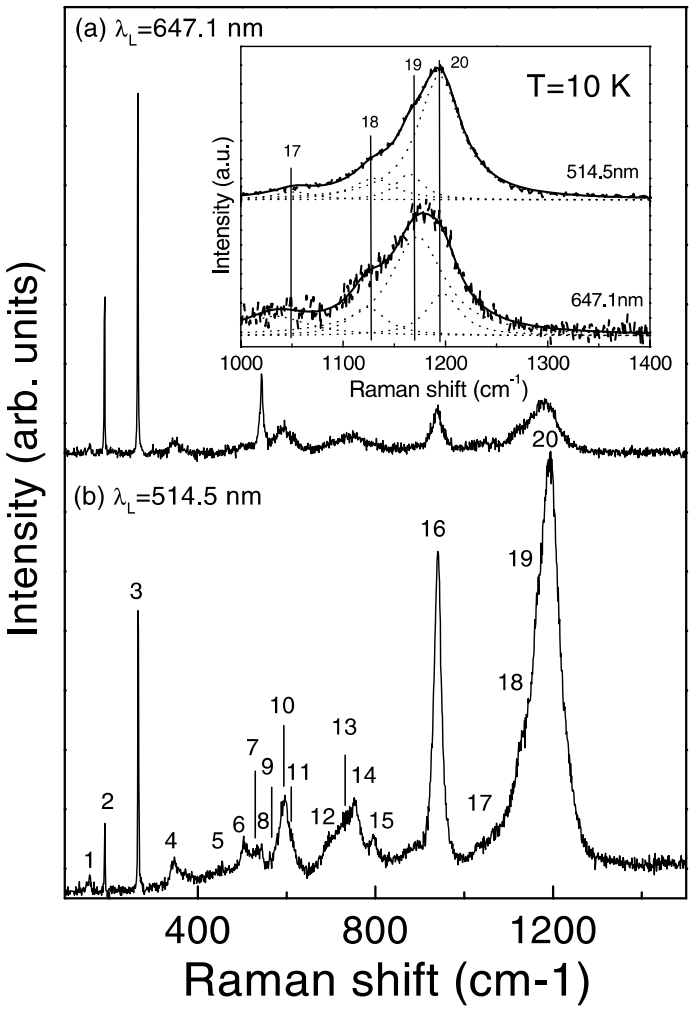

Fig. 4. The (*cc*) polarized Raman spectra of $SrCuO_2$ at 10 K for (a) 647.1 nm and (b) 514.5 nm excitation. Inset: Raman spectra measured with 647.1 nm and 514.5 nm lines at 10 K in the spectral range 1000–1400 cm^{-1}, deconvoluted by Lorentzians.

CuO_2 sheets in Nd_2CuO_4. To best of our knowledge there is no experimental data about energy gap of $SrCuO_2$. We attempted to extract some information from optical conductivity spectra of the $Ca_{0.85}Sr_{0.15}CuO_2$ crystal. We have obtained the main conductivity peak at 1.6 eV and a less prominent tail at 2.1 eV by deconvolution of the optical conductivity spectra of $Ca_{0.85}Sr_{0.15}CuO_2$ given in Fig. 1(e) of Ref. [16], who obtained their conductivity spectra by Kramers–Kronig analysis of the reflectivity data, measured at room temperature with the polarization parallel to the Cu–O chains. Since the substitution of Ca for Sr atoms produces crystal structure transition from orthorhombic to tetragonal and a corresponding change of electronic structure, it was not possible to use these data as a gap values of $SrCuO_2$. Instead, we measured the dielectric function and optical reflectivity of $SrCuO_2$ in the visible and UV spectral range. The dielectric function ε_2 of $SrCuO_2$ is shown in Fig. 5. These spectra were computed from the measured Fourier coefficients using the equations for an isotropic case. Consequently, ε_2 represents a complicated average of the projections

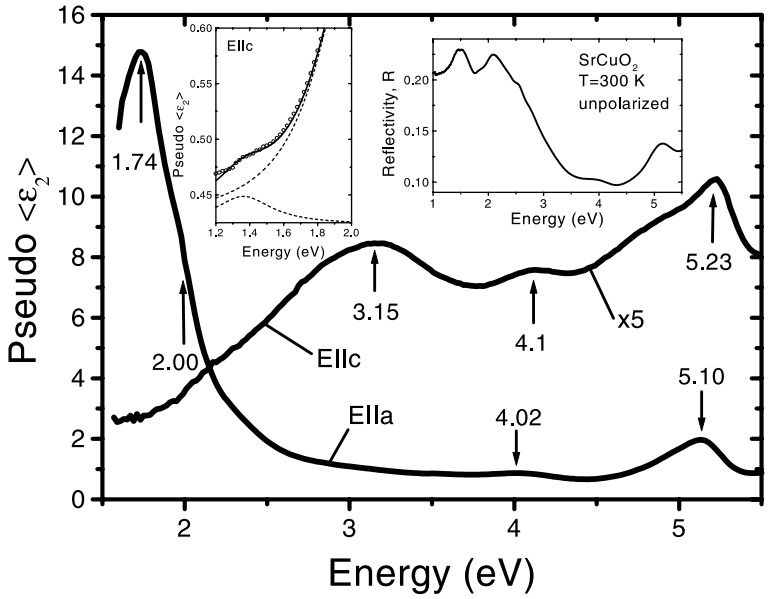

Fig. 5. Room temperature imaginary part (ε_2) of the pseudodielectric function of $SrCuO_2$. The spectra of the (0 1 0) surface taken with a-axis ($E \| a$) and c-axis ($E \| c$), parallel to the plane of incidence. Inset left: The $\varepsilon_2(\omega)$ spectra in the 1.2–1.8 eV range for $E \| c$ polarization. Inset right: unpolarized room temperature reflectivity spectra of $SrCuO_2$ in the 1–5.5 eV range.

of the dielectric tensor on the sample surface. Bands with the energies of 3.15, 4.1 and 5.23 eV were found for the c axis, and at about 1.74, 2.0, 4.02, and 5.1 eV for the a-axis in the plane of incidence, respectively. By comparison of ellipsometric data in Fig. 5 with optical reflectivity spectra shown in the right inset of Fig. 5, we concluded that dielectric functions coincide with reflectivity spectra in the spectral range from 1.6 to 5.5 eV. In order to check from which polarization originate the lowest energy maxima in optical reflectivity spectra at about 1.5 eV we measured dielectric functions in 1.2–1.8 eV range, also (left Inset of Fig. 5). We found that only for $E \| c$ polarization exists a weak structure at about 1.4 eV. The position of this line is obtained by a Lorentzian deconvolution. We conclude that the lowest energy gap in $SrCuO_2$ (E_0) is at about 1.4 eV (1.74 eV) for $E \| c$ ($E \| a$) polarization.

According to the spectra in Fig. 4, the enhancement of the Raman-forbidden modes appears at higher energies than the gap value. Namely, in the case of the 647.1 nm excitation, Raman-allowed Ag modes at 190, 265 and 544 cm^{-1} are the dominant structures. With an increase in excitation energy to 514.5 nm, additional structures enhance resonantly and new modes, superimposed on a wide background, appear. The frequencies and the assignment of all observed modes are given in Table 2. A more detailed analysis indicates that the Raman-allowed A_g modes in combination with the LO modes also contribute to the two-phonon spectra. For the modes at 796 cm^{-1} (A) and 1168 cm^{-1} (B) no corresponding combination of modes has been found, and we presume that they originate from zone-edge phonons.

The highest intensity mode at about 1195 cm^{-1} is asymmetric due to superposition of several modes. We fitted this structure with four Lorentzians in order to determine frequencies at which maxima occur (upper inset in Fig. 4). For the 514.5 nm line, the dominant contribution to this mode comes from $2LO_3$. Using the 647.1 nm excitation, this mode becomes weaker than the mode at about 1170 cm^{-1} (B), giving the impression that its frequency decreases by lowering the excitation energy.

Table 2
Frequencies (in cm^{-1}) and assignment of modes observed for (*cc*) polarization at T = 10 K

Number of peaks	Frequency	Remark
1	156	LO_1
2	190	A_{g1}
3	265	A_{g2}
4	347	LO_2
5	455	$A_{g1} + A_{g2}$
6	503	$LO_1 + LO_2$
7	530	$2A_{g2}$
8	544	A_{g3}
9	562	A_{g4}
10	596	LO_3
11	610	$A_{g2} + LO_2$
12	694	$2LO_2$
13	733	$A_{g1} + A_{g3}$
14	755	$LO_1 + LO_3$
15	796	A
16	941	$LO_2 + LO_3$
17	1040	$2LO_3 - LO_1$
18	1130	$A_{g2} + LO_3$
19	1168	B
20	1195	$2LO_3$

Having above in mind, we conclude that the 2LO overtone processes are not resonantly enhanced with a laser line energy (1.91 eV) near the lowest energy gap but with a laser energy close to the energies at which the light absorption is significantly increased (light absorption maxima for higher energy transitions). This effect, observed for the first time in II–IV Mg_2X (X = Si, Ge, Sn) type semiconductors [17–19], is attributed to spatial dispersion effects arising from the finite wave-vectors of phonons and/or the incident and scattered electromagnetic radiation. As it is shown also in Ref. [19], the strength of resonance in Mg_2X at E_0 is weaker than that at higher energy transitions, which is explained by the weaker electron-phonon interaction at E_0.

In 1D antiferromagnetic $S = 1/2$ systems, the excitation spectrum consists of magnon (more precisely spinon) continuum that builds up at nonzero momentum (largest contribution is at zone boundary). Therefore, some contribution in form of two-spinon continuum might be expected in the Raman spectra. However, in the Raman as well as in the infrared spectra of $SrCuO_2$, measured up to 6000 cm^{-1} ($J \sim 1500$ cm^{-1}), we did not find any feature which could be assigned as magnetic in origin, as in the case of Sr_2CuO_3 [20]. The reason for this is probably very small spectral weight of these excitations. Besides, the two-spinon Raman intensity, in perfect 1D case, is expected to be largest at small energies and continuously decreases towards higher energies. There, at low energies, we see strong two-phonon continuum that mask week two-spinon continuum. At the other hand, the magnetic structure of $SrCuO_2$ is of zigzag spin-chain type [21–24], different to that of Sr_2CuO_3, which also might be the reason for the different Raman and IR spectra in these two compounds.

In conclusion, we presented the polarized FIR reflectivity, Raman scattering spectra and ellipsometric as well as optical reflectivity results of single crystal $SrCuO_2$. In addition to Raman-allowed modes, the Raman-forbidden–infrared-allowed B_{1u} LO modes are observed for polarization parallel to the *c*-axis. These modes are resonantly enhanced for a laser energy close to the electronic transition of higher energy gaps. This effect could be either explained by the exciton-mediated multiphonon Raman scattering or attributed to the spatial dispersion effects arising from the finite wave vectors of the phonons and/or the incident and scattered electromagnetic radiation. Resonant Raman scattering in charge transfer 2D insulating cuprates [15,25] shows that IR-modes and their overtones resonate much more strongly near the optical absorption edge. In $SrCuO_2$ (1D cuprate) IR modes resonate at energies higher than the lowest energy gap. It means that there are significant differences between the electronic structure of $SrCuO_2$ and other 2D cuprates.

Acknowledgements

We thank Prof. E. Anastassakis for helpful discussion. Z.V.P. acknowledges support from Alexander von Humboldt Stifting-Bonn and from the Research Council of the K.U. Leuven and DWTC. The work at the K.U. Leuven is supported by the Belgian IUAP and Flemish FWO and GOA Programs. M.J.K thanks Roman Herzog-AvH for partial financial support.

References

[1] Z. Hiroi, M. Takano, M. Azuma, Y. Takeda, Y. Bando, Physica C 185–189 (1991) 523.
[2] C. Kim, A.Y. Matsura, Z.X. Shen, N. Motoyama, H. Eisaki, S. Uchida, T. Tohoyama, S. Maekawa, Phys. Rev. Lett. 77 (1996) 4054.
[3] C. Kim, Z.X. Shen, N. Motoyama, H. Eisaki, S. Uchida, T. Tohoyama, S. Maekawa, Phys. Rev. B 56 (1997) 15589.
[4] N. Motoyama, H. Eisaki, S. Uchida, Phys. Rev. Lett. 76 (1996) 3212.
[5] M. Matsuda, K. Katsumata, K.M. Kojima, M. Larkin, G.M. Luke, J. Merrin, B. Nachumi, Y.J. Uemura, H. Eisaki, N. Motoyama, S. Uchida, G. Shirane, Phys. Rev. B 55 (1997) R11953.
[6] O.V. Misochko, S. Tajima, C. Urano, H. Eisaki, S. Uchida, Phys. Rev. B 53 (1996) R14733.
[7] M.V. Abrashev, A.P. Litvinchuk, C. Thomsen, V.N. Popov, Phys. Rev. B 55 (1997) 9136.
[8] M.V. Abrashev, A.P. Litvinchuk, C. Thomsen, V.N. Popov, Phys. Rev. B 55 (1997) R8638.
[9] Chr.L. Taske, Hk. Müller-Buschbaum, Z. Anorg. Allg. Chem. 377 (1970) 144.
[10] Matsushita, Y. Oyama, M. Hasegawa, H. Takei, J. Solid, State Chem. 114 (1994) 289.
[11] X. Zhou, M. Cardona, W. König, J. Zegenhagen, Z.X. Zhao, Physica C 282–287 (1997) 1011.
[12] Z.V. Popović, M.J. Konstantinović, S.N. Miličić, A. Vietkin, A. Revcolevschi, Balkan Phys. Lett. 7 (1999) 45.
[13] M. Yoshida, S. Tajima, N. Koshizuka, S. Tanaka, S. Uchida, T. Itoh, Phys. Rev. B 46 (1992) 6505.
[14] I. Ohana, D. Heiman, M.S. Dresselhaus, P.J. Picone, Phys. Rev. B 40 (1989) 2225.
[15] M. Reedyk, C. Thomsen, M. Cardona, J.S. Xue, J.E. Greeden, Phys. Rev. B 50 (1994) 13762.
[16] Y. Tokura, S. Koshihara, T. Arima, H. Takagi, S. Ishibashi, T. Ido, S. Uchida, Phys. Rev. B 41 (1990) 11657.
[17] E. Anastassakis, C.H. Perry, Phys. Rev. B 4 (1971) 1251.
[18] E. Anastassakis, E. Burstein, in: M. Balkanski (Ed.), Light Scattering in Solids, Flammarion Sciences, Paris, 1971, p. 52.
[19] S. Onari, E. Anastassakis, M. Cardona, in: M. Balkanski, R.C.C. Leite, S.P.S. Porto (Eds.), Light Scattering in Solids, Flammarion Sciences, Paris, 1976, p. 54.
[20] H. Suzuura, H. Yasuhara, A. Furusaki, N. Nagaosa, Y. Tokura, Phys. Rev. Lett. 76 (1996) 2579.
[21] Z.V. Popović, V.A. Ivanov , M.J. Konstantinović, A. Cantarero, J. Martinez-Pastor, D. Olguin, M.I. Alonso, M. Garriga, O.P. Khuong, A. Vietkin, V.V. Moshchalkov, unpublished results.
[22] S.R. White, I. Affleck, Phys. Rev. B 54 (1996) 9862.
[23] T. Tonegawa, I. Harada, J. Phys. Soc. Jpn. 56 (1987) 2153.
[24] N. Maeshima, K. Okunichi, Phys. Rev. B 62 (2000) 934.
[25] R. Liu, M.V. Klein, D. Salamon, S.L. Cooper, W.C. Lee, S.W. Cheong, D.M. Ginsberg, J. Phys. Chem. Solids 54 (1993) 1347.